Formulation of Resonance Frequency for Dual band Slotted H-shaped Microstrip Antenna

Amit A. Deshmukh
DJSCOE, Vile Parle (W)
Mumbai 400 056, India

Priyanka Thakkar
DJSCOE, Vile Parle (W)
Mumbai 400 056, India

Sneha Lakhani
DJSCOE, Vile Parle (W)
Mumbai 400 056, India

Mayank Joshi
DJSCOE, Vile Parle
(W), Mumbai 400 056
India

K. P. Ray
SAMEER, I.I.T.
Campus, Powai,
Mumbai 400 076,

ABTSRACT
The resonance frequency formulation for hexagonal microstrip antenna using its equivalence to circular microstrip antenna is proposed for fundamental and higher order modes and it gives closer agreement with simulated results. The compact variations of H-shaped microstrip antennas in its fundamental mode are proposed. The dual band H-shaped microstrip antenna realized by cutting a U-slot or pair of rectangular slots is proposed. They give dual band response with broadside radiation pattern. To understand the mode introduced by the slot, the analysis for slot cut H-shaped antennas is carried out by studying their surface current distributions out over a wide frequency range. It was observed that neither of the U or rectangular slots introduce any mode but they alter the higher order mode resonance frequency of the patch and along with the fundamental mode realizes dual frequencies. By studying the surface current distributions, a formulation of the resonant length for the slot mode is proposed. The frequencies calculated using them agree well with the simulated results with an error of less than 5% over the entire slot length range.

Keywords
Circular microstrip antenna, H-shaped microstrip antenna, Compact H-shaped microstrip antenna, dual band H-shaped microstrip antenna

1. INTRODUCTION
The microstrip antenna (MSA) is low profile and planar configurations but have lower operating bandwidth (BW) and larger patch size in UHF range [1 – 3]. Different techniques have been reported to increase the BW and to reduce the patch size [4 – 6]. The commonly used shapes of the radiating patch in MSA are Rectangular, Circular and Equilateral triangular and the equations for the resonance frequencies of these shapes are reported [1 – 3]. A new H-shaped patch is reported which is derived from the Rectangular shape [1]. Since the H-shaped MSA (HMSA) was derived from the rectangular MSA (RMSA) the resonance frequency formulation for the given dimensions of the HMSA was derived from the RMSA [1]. The field distribution for the HMSA at the fundamental mode was found to be similar to the field distribution of the circular MSA and hence using its equivalence to the circular patch, the formulation of resonance frequency for HMSA has been proposed [7]. A dual band microstrip antenna (MSA) is realized either by placing an open circuit nearly quarter wavelength or short circuit nearly half wavelength stub on the edges of the patch [8, 9]. The stub offers capacitive and inductive impedance around the resonance frequency of MSA and realizes dual band response. However since the stub is placed on the edges of the patch it increases the overall patch area and the radiation from the stub affects the radiation pattern of the MSA. The dual band response is also realized by cutting the slot at an appropriate position inside the patch [10 – 12]. Since the slot is cut inside the patch it neither increases the patch size nor it largely affects the radiation pattern of the patch and hence it is more frequently used technique to realize dual band MSA. The dual band H-shaped MSAs realized by cutting either pair of rectangular slots or the U-slot is reported [7]. In all these slot cut MSAs, the general understanding is that when the slot length is either half wave or quarter wave in length, it introduces a mode near the fundamental resonance frequency of the patch and realizes dual band response. However these half and quarter wave length approximations of slot length against the frequency does not give closer results for different slot length and its position inside the patch.

In this paper, using the equivalence of the HMSA with that of the CMSA, the resonance frequency formulation for the fundamental as well as second order mode of HMSA is proposed. The frequencies obtained using the proposed formulation agrees within 5% with that of the simulated values at fundamental as well as higher order modes. The formulations obtained using this method also agrees closely with the simulated results for RT-duroid substrate at different frequencies. The compact variations of HMSA by placing the shorting posts along zero field line are proposed. The dual band configurations of HMSA by cutting a pair of rectangular slots or U-slot inside the patch are proposed. These dual band configurations give broadside radiation pattern at the dual frequencies. The dual band response in the pair rectangular slots cut H-shaped MSAs was studied for different slot dimensions and their positions inside the patch. The surface current distributions generated using the IE3D software was studied. They were compared with the current distributions of the H-shaped MSA. It was observed that the slot does not introduce any mode but alters the resonance frequency of higher order TM_{21} mode and along with the fundamental mode, realizes dual band response. By studying the surface current distributions of rectangular slot cut H-shaped MSAs, the formulation of resonance frequency for dual band H-shaped MSA is proposed. The frequency obtained using these proposed formulations agrees well

with the simulated results with an error of less than 5% over the slot length range. All these MSAs were first analyzed using the IE3D software [13] followed by experimental verification in dual band HMSAs. The glass epoxy substrate (ε_r = 4.3, h = 1.6 mm, tan δ = 0.02) is used for the simulations as well as the measurements. The HMSAs are fed using the SMA connector of inner wire diameter of 0.12 cm.

2. FORMULATION OF RESONANCE FREQUENCY FOR H-SHAPED MSA

The regular H-shaped MSA is shown in Figure 1(a). In regular H-shaped MSA, all the side lengths have equal lengths. For the dimensions shown in Figure 1(a), the first order resonance frequency of the HMSA is 915 MHz as shown in its surface current distributions in Figure 1(b). The surface currents show one half wave length variations, which is similar to the current distributions of TM_{11} mode in CMSA. Due to this similarity between HMSA and CMSA, the resonance frequency formulation for HMSA is derived using frequency formulation for CMSA as given below.

$$a_H = 2.598S^2 \quad (1)$$

$$a_C = \pi r_c^2 \quad (2)$$

Equating the two areas gives,

$$r_c = S\sqrt{2.598/\pi} \quad (3)$$

$$f_r = \frac{K_{mn}c}{2r_c\pi\sqrt{\varepsilon_r}} \quad (4)$$

$$\%\,\text{error} = \left(f_{cmsa} - f_{hmsa}\right)/f_{hmsa} \quad (5)$$

where,
a_H = area of HMSA,
a_C = area of CMSA,
r_C = equivalent radius of CMSA
K_{mn} = 1.84118 (TM_{11} mode)

The resonance frequencies obtained using the IE3D simulation for S = 2 to 6 cm and that obtained using equivalent CMSA whose radius is calculated by using above equations, are shown in Figure 2. The % error between the HMSA frequency and equivalent CMSA frequency is calculated by using equation (5). For the entire range a close agreement between the two results is obtained. The current distribution at next frequency (second order mode) for HMSA is shown in Figure 1(c). The surface current distribution at the second order mode of HMSA is similar to the current distribution at the TM_{21} mode of CMSA. Thus the resonance frequency formulation at the next mode is obtained by using its CMSA equivalence. The equation (4) is used to calculate the same with K_{mn} = 3.05424. The frequency at next mode of HMSA and that obtained using its CMSA equivalence are shown in Figure 3. For different values of S, an error of less than 5% is obtained.

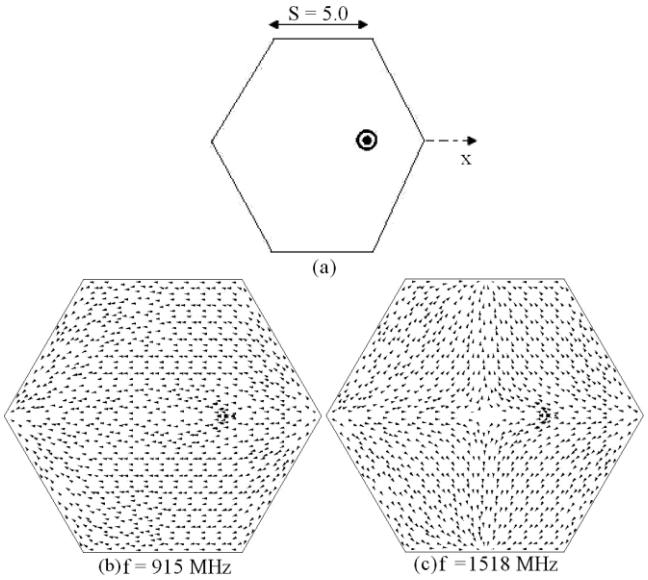

Figure 1 (a) HMSA and its (b, c) Surface current distribution at first two frequencies

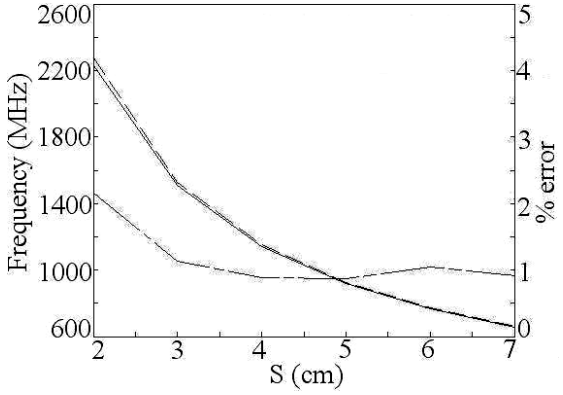

Figure 2 Resonance frequency and % error plots for HMSA for different S at first order mode, (——) HMSA, (– – –) Equivalent CMSA, (— — —) % error

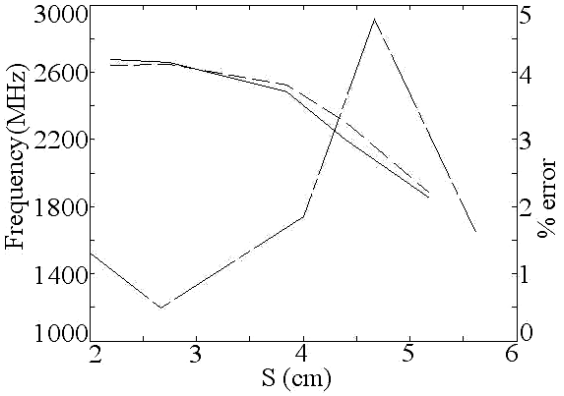

Figure 3 Resonance frequency and % error plots for HMSA

for different S at second order mode, (——) HMSA, (– – –) Equivalent CMSA, (——–——) % error

3. COMPACT HMSAs

The compact HMSAs are realized by placing the shorting posts along the zero field line at the first mode of HMSA. The resonance frequency of HMSA is 915 MHz with a BW of 12 MHz. Since the field is symmetrical across the feed point axis, by removing the bottom half of HMSA, a compact half HMSA is realized as shown in Figure 4(b). This HMSA resonates at 928 MHz with a BW of 11 MHz. Since the area of the MSA is reduced its resonance frequency has increased. By placing the shorting posts along the zero field line of HMSA, shorted half HMSA is realized as shown in Figure 4(c). The resonance frequency of this configuration is 926 MHz. By using its symmetry along the feed point axis a super compact half shorted half HMSA is obtained as shown in Figure 4(d). This configuration resonates at 936 MHz. The results for all these compact variations of HMSA are summarized in Table 1.

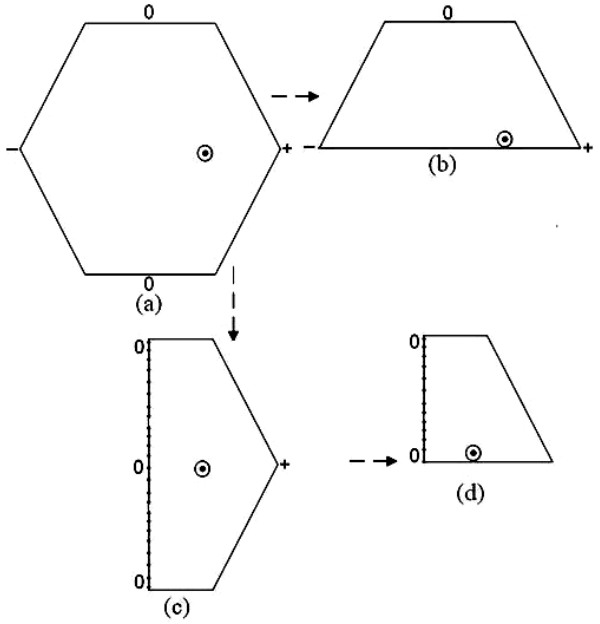

Figure 4 (a) HMSA, (b) half HMSA, (c) shorted half HMSA and (d) half shorted half HMSA

Table 1. Comparison between various compact HMSA configurations

HMSA shown in	f_r (MHz)	BW (MHz)	Area (cm^2)	Feed point (cm)
Figure 4(a)	915	10	65	2.2
Figure 4(b)	928	9	32.5	1.37
Figure 4(c)	926	15	32.5	1.36
Figure 4(d)	936	8	16.25	0.76

The area reduction by a factor of 75% is realized in super compact half shorted half HMSA. The radiation pattern for HMSA is in the broadside direction as shown in Figure 5(a). The E and H-planes are aligned along $\Phi = 0^0$ and 90^0, respectively. In shorted HMSAs, since the field distributions along the periphery of the shorted HMSA is changed, the pattern shows higher cross polarization levels in the E and H-planes as shown in Figure 5(b).

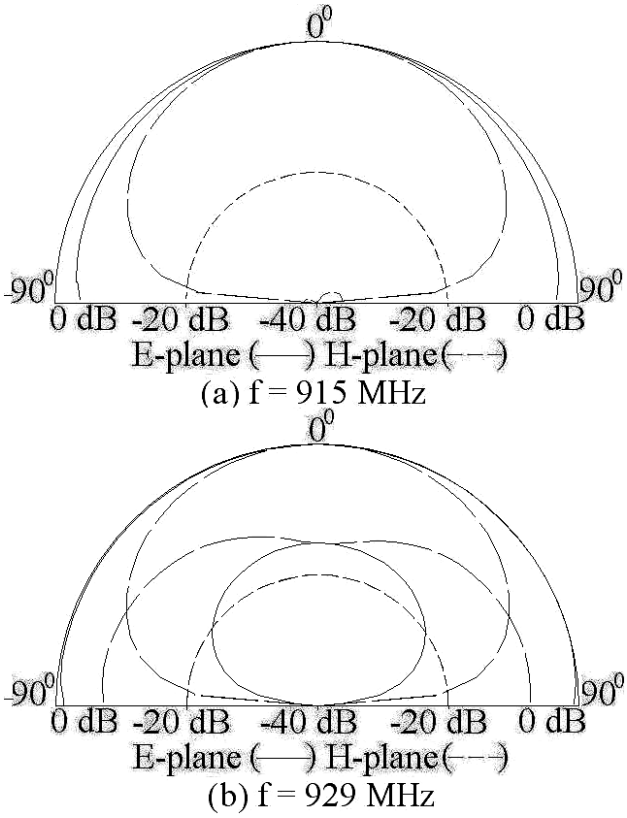

Figure 5 Radiation pattern for (a) HMSA and (b) half shorted half HMSA

4 DUAL BAND H-SHAPED MSAs

The dual band pair of rectangular slots cut HMSA is shown in Figure 6(a). The pair of rectangular slots is cut on one of the patch edges. Its length is taken to be nearly quarter wave in length at the required dual frequencies. The slot width is taken to be 0.2 cm. Since the shape of this HMSA resembles to the letter 'E', this configuration is called as E-shaped HMSA. To realize the impedance matching, the feed point is located on the other side of the slots. For the given dual frequencies, slot dimensions and separation between them is optimized. The optimized return loss (S_{11}) plots are shown in Figure 6(b). For slot length of 2 cm, the simulated dual frequencies and BW's are 898 and 1186 MHz and 15 and 12 MHz, respectively. The measured frequencies and BW's are 890 and 1172 MHz and 14 and 13 MHz, respectively. In the measurements the size of the ground plane is taken to be more than six times the substrate thickness in all direction with respect to the patch dimensions so as to realize the effect of infinite ground plane. The measured radiation pattern at the dual frequencies is in the broadside direction with cross- polarization levels less than 15 dB as compared to that of the co-polar levels as

shown in Figure 7(a, b). The photo of the fabricated prototype of E-shaped HMSA is shown in Figure 8.

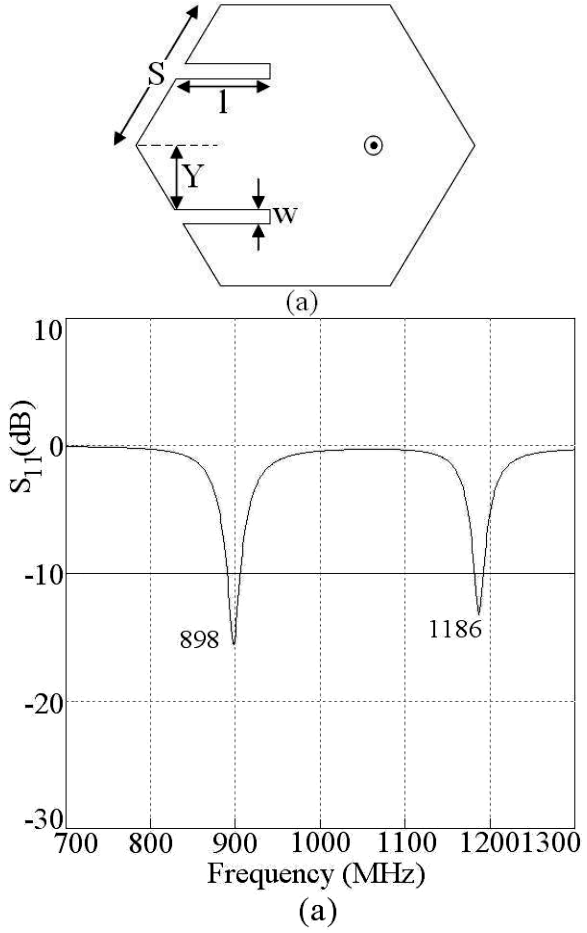

Figure 6 (a) E-shaped HMSA and its (b) simulated return loss plots

The dual frequency response is also realized by cutting a pair of rectangular slots inside the HMSA as shown in Figure 9(a). In this configuration the slot are taken to be nearly half wave in length. By optimizing the slot length, the dual band response is realized and the simulated return loss plots are shown in Figure 9(b). The simulated dual frequencies and BW's are 915 and 1009 MHz and 18 and 13 MHz, respectively. The measured frequencies and BW's are 901 and 1018 MHz and 15 and 11 MHz, respectively. The radiation pattern at the dual frequencies is in the broadside direction with cross-polarization levels less than 20 dB as compared to that of the co-polar levels as shown in Figure 10(a, b). Since the slots are cut symmetrical to the feed point axis this dual band HMSA shows lower cross polarization levels as compared to the dual band E-shaped HMSA. The photo of the fabricated prototype of pair of rectangular slots cut HMSA is shown in Figure 11. The dual band HMSA can also be realized by cutting the U-slot in the centre of the HMSA as shown in Figure 12. In this configuration, the inner U- slot length nearly equals half the wavelength.

In the dual band slot cut MSA, for the given slot frequency, the slot length is taken to be either quarter wave or half wave in length. However this simpler approximation does not give closer results for different slot dimensions and their position inside the patch. Therefore an in-depth analysis of slot cut MSAs over a wide frequency range is needed. Here the analysis for E-shaped HMSA is presented.

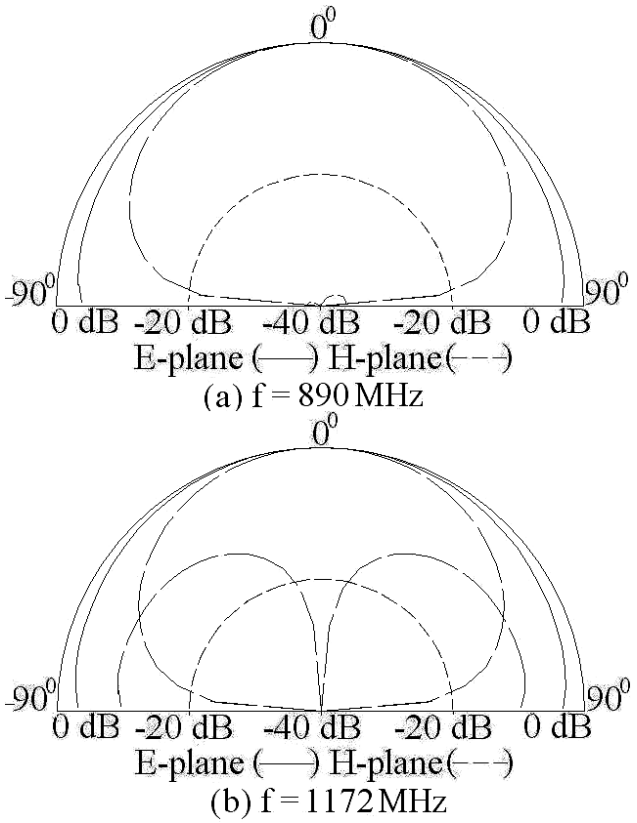

Figure 7 (a, b) Radiation pattern at dual frequencies for E-shaped HMSA

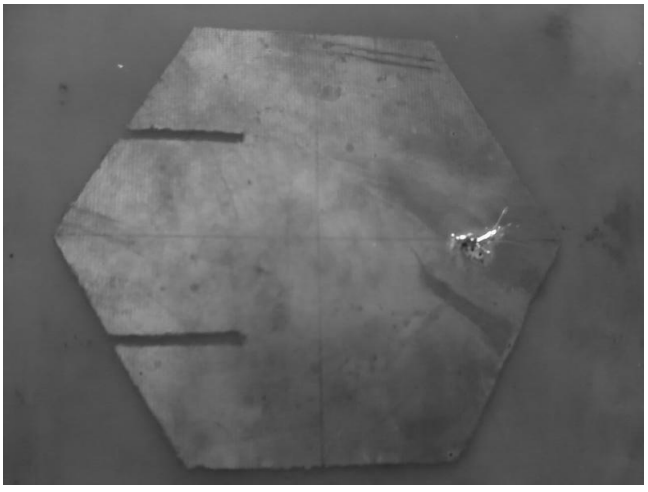

Figure 8 Fabricated prototype of E-shaped HMSA

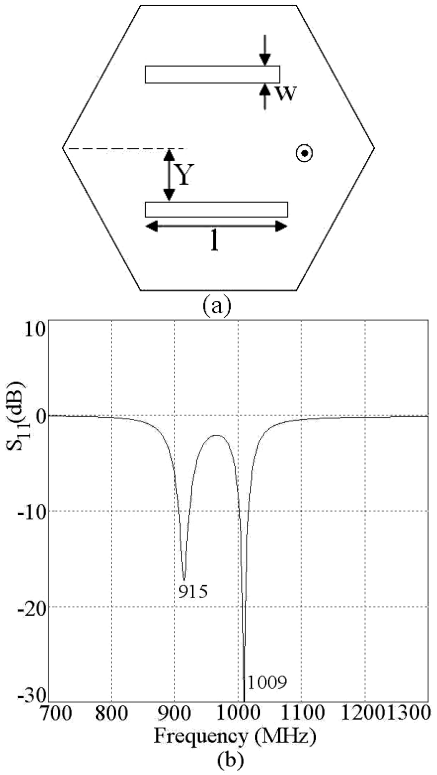

Figure 9 (a) Pair of rectangular slot cut HMSA and its (b) Simulated return loss plots

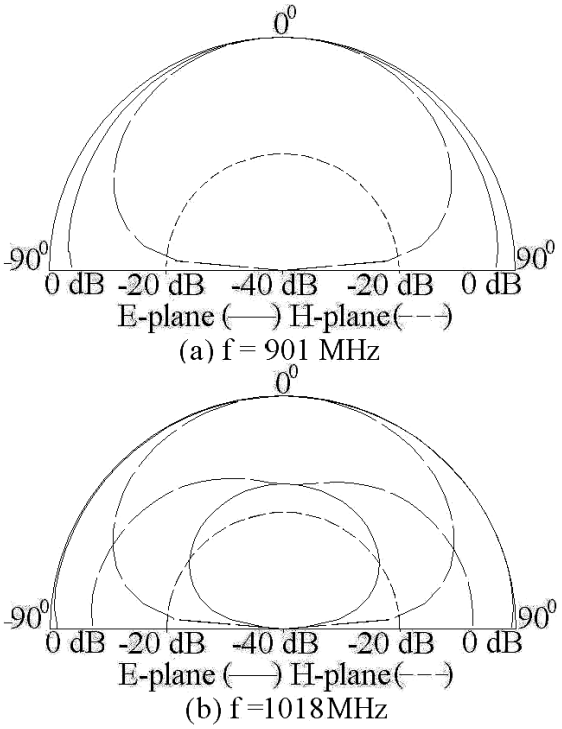

Figure 10 (a, b) Radiation pattern at dual frequencies for E-shaped HMSA

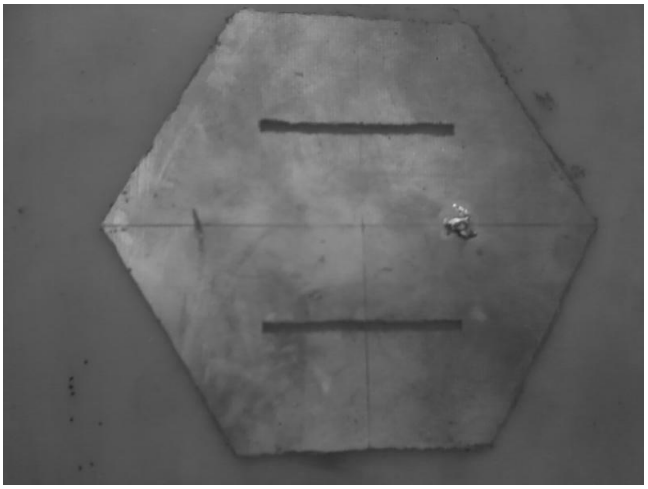

Figure 11 Fabricated prototype of pair of rectangular slots cut HMSA

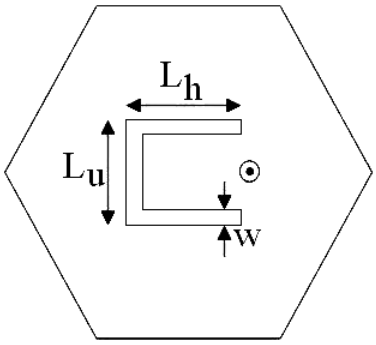

Figure 12 Dual band U-slot cut HMSA

5. MODAL ANALYSIS OF DUAL BAND HMSAs

The resonance curve plot for the HMSA having S = 5 cm, is shown in Figure 13. The surface current distributions for the first two modes of this HMSA (TM_{11} and TM_{21}) are shown in Figure 1(b, c). The pair of rectangular slots is cut inside this HMSA to realize E-shaped HMSA and the current distribution and simulated radiation patterns for each of the slot length were studied. For the slot length of 2.0 cm, the current distributions at the dual frequencies for E-shaped HMSA is shown in Figure as shown in Figure 14(a, b). The resonance curve plot for the E-shaped MSA is shown in Figure 12. As seen from the resonance curve plot that the pair of slots has reduced the second order TM_{21} mode resonance frequency. This frequency has come closer to fundamental TM_{11} mode frequency of HMSA. Also the surface current distribution at the second frequency of E-shaped HMSA is similar to the current distribution at the TM_{21} mode frequency of the HMSA. Thus it is inferred from the resonance curve and the current distribution that the slots does not introduce any mode but modifies the higher order TM_{21} mode frequency and along with the fundamental TM_{11} frequency realizes dual band response. The radiation pattern at the fundamental mode of HMSA (TM_{11}) is in the broadside direction as shown in Figure 5(a) whereas at the

TM_{21} mode it is in the conical direction as shown in Figure 14(c). However as the slot modifies the directions of the surface currents at the higher order mode, the radiation pattern at the dual frequencies in E-shaped HMSA is in the broadside direction as shown in Figure 7(a, b).

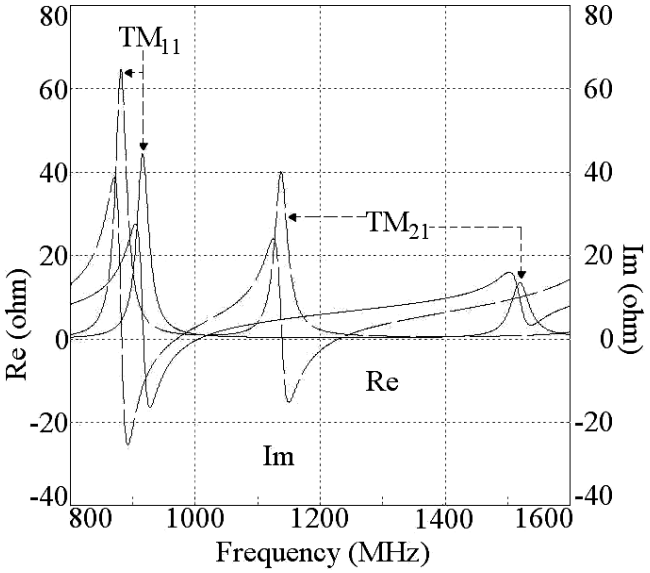

Figure 13 Resonance curve plots for HMSA (———) and E-shaped HMSA (— — —)

By studying the surface current distribution for the E-shaped HMSA, a formulation of the resonant length at the dual frequencies is proposed. By modifying the effective patch radius with respect to the slot length the formulation of resonant length at modified TM_{11} and TM_{21} modes are realized. At the first frequency the resonant length formulation is obtained by using equations (6) to (9). The r is the effective radius of the equivalent CMSA obtained using equation (3). The frequency is calculated using equation (3). The % error between the calculated and simulated frequencies which is obtained using IE3D software is calculated using equation (9). For Y = 1 to 3.5 cm, the frequencies and % error are shown in Figures 15 and 16.

At f_1,

$$r = 0.909S \quad (6)$$

$$r_{e1} = r + 2l\sin\left(\pi/21r\right) \quad (7)$$

$$f_1 = 1.84118c \Big/ 2r_{e1}\pi\sqrt{\varepsilon_r} \quad (8)$$

$$E = \left(f_{ie3d} - f_1 \Big/ f_{ie3d}\right)100 \quad (9)$$

where, $c = 3 \times 10^8$ m/s,
r_{e1} = effective patch radius due to the slot
f_1 = calculated first frequency
f_{ie3d} = simulated frequency
E = % error between the two frequencies

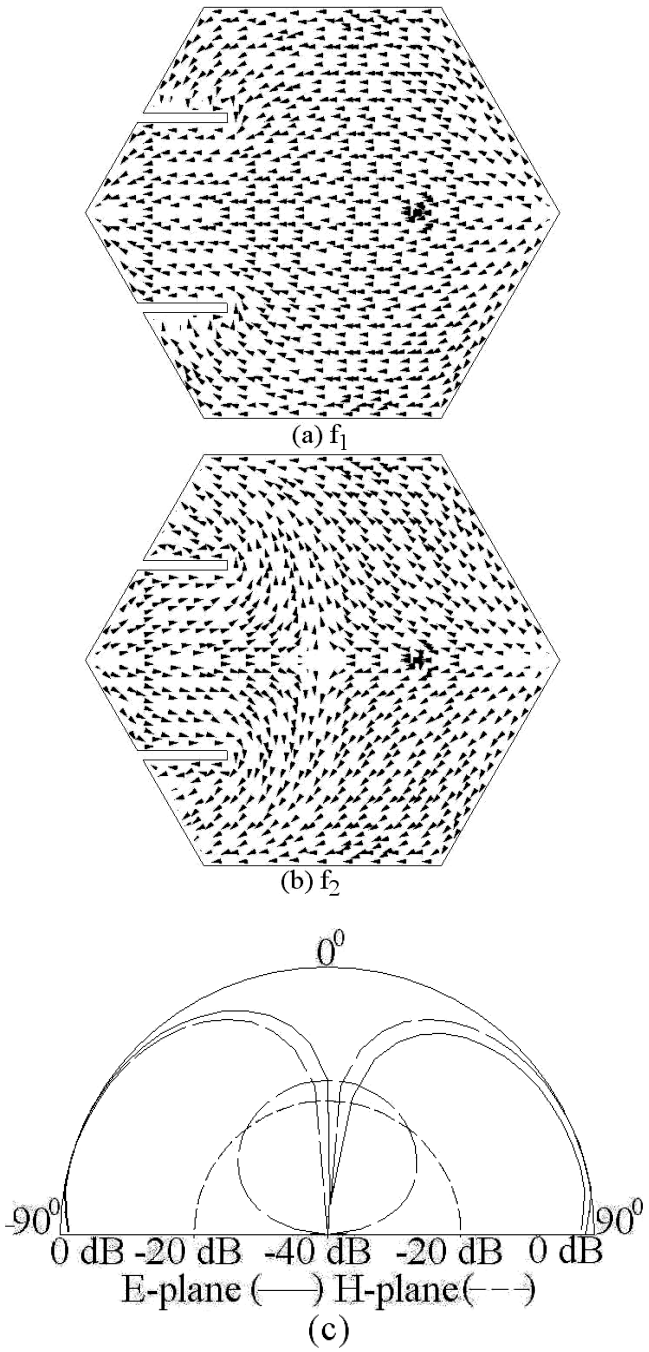

Figure 14 (a, b) Surface current distribution at dual frequencies and (c) radiation pattern at TM_{21} mode for HMSA

For all the values of Y, an error less than 5% over the entire slot length range is obtained. Similarly by studying the surface current distributions the formulation of resonant length at second frequency is obtained as given in equations (10) to (14). The perturbation in TM_{21} mode resonant length is smaller for smaller slot length whereas it increases for higher slot length. This non-linear variation in the perturbation is modelled by using the

weighting function A. The equation for A is derived based on the modified TM_{21} mode resonance frequency with respect to slot length. The resonance frequency is calculated by using equation (13) and the % error between the calculated and simulated frequency is calculated using equation (14). For Y = 1.0 to 3.5 cm, they are plotted in Figures 17 and 18. For all the values of Y, an error less than 5% over the varying slot length is obtained.

At f_2,

$$r = 0.909S \quad (10)$$

$$r_{e1} = r + 2\,l\,A \quad (11)$$

$$A = \left(l/2r\right)\sin\left(\pi l/2r\right) \quad (12)$$

$$f_2 = 3.05424c \Big/ 2r_{e1}\pi\sqrt{\varepsilon_r} \quad (13)$$

$$E = \left(f_{ie3d} - f_2 \Big/ f_{ie3d}\right)x100 \quad (14)$$

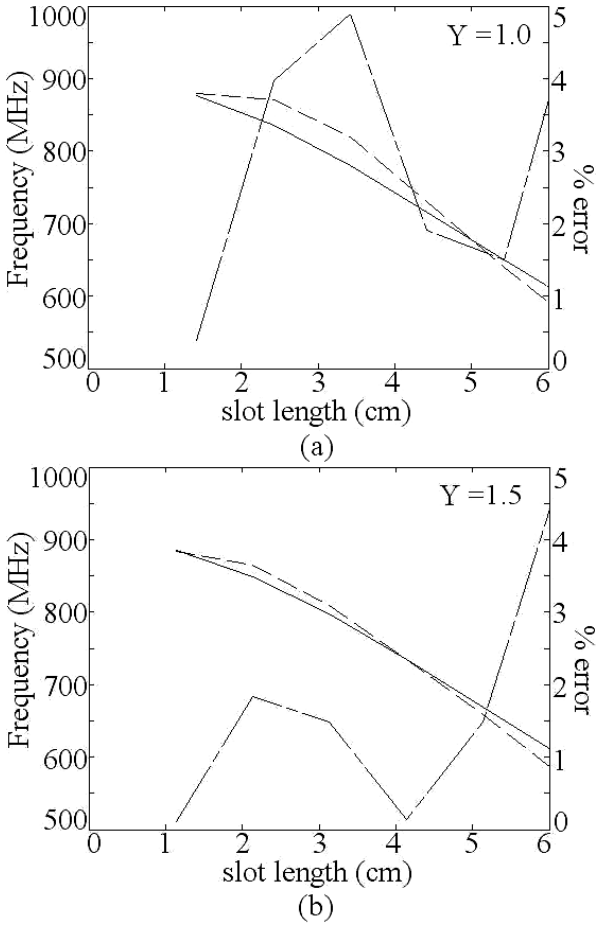

Figure 15 (a, b) Resonance frequency and % error plots for E-shaped HMSA, (—) IE3D, (– –) calculated, (— – —) % error

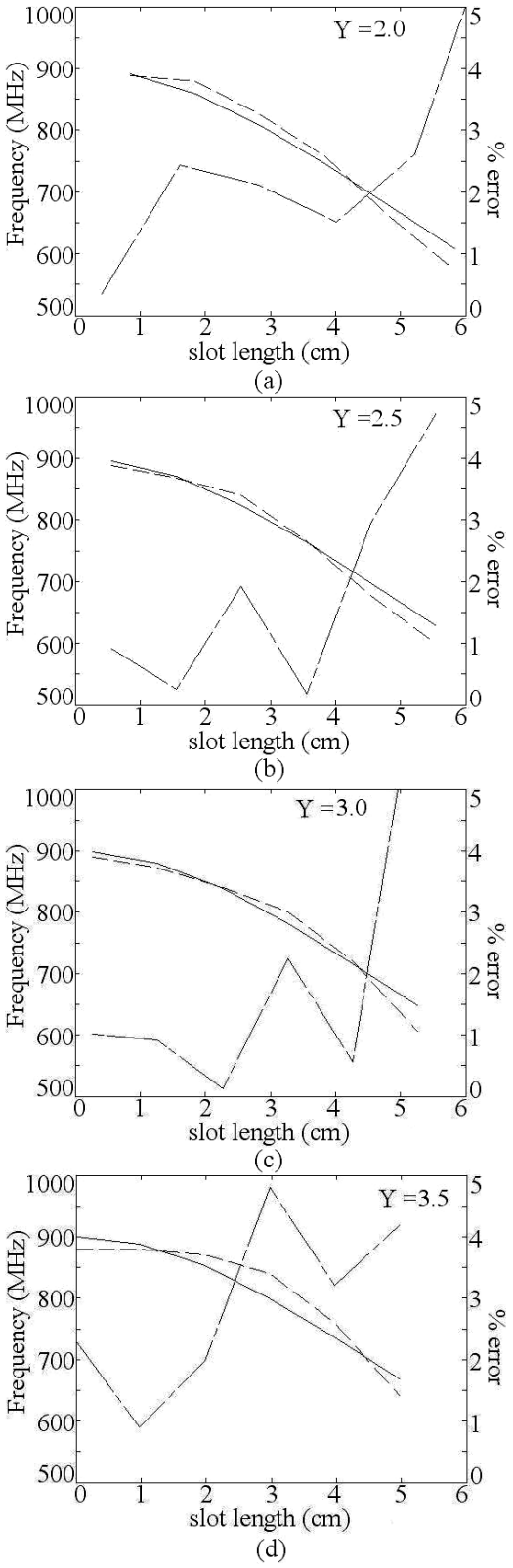

Figure 16 (a – d) Resonance frequency and % error plots for E-shaped HMSA, (—) IE3D, (– –) calculated, (— – —) % error

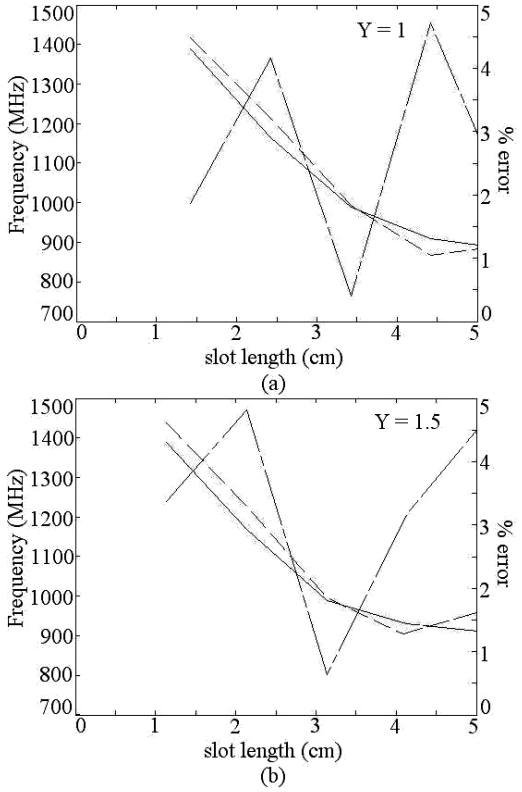

Figure 17 (a, b) Resonance frequency and % error plots at f_2 for E-shaped HMSA, (—) IE3D, (– –) calculated, (— - —) % error

Thus for all the values Y, the % error is less than 5% over the entire slot length range. The above formulations for the HMSA resonance frequency as well as for the slot resonant length (modified TM_{21} mode) in E-shaped HMSA have been verified for the RT-duroid substrate and also at the different frequencies. In all the cases a % error less than 5% is obtained.

6. CONCLUSIONS

The resonance frequency formulation for HMSA using its equivalence to CMSA is proposed. The frequencies calculated using the proposed formulation closely agrees with HMSA frequencies at the fundamental as well as the second order mode. The compact variations of shorted HMSAs are proposed. They reduces the patch area with nearly the same resonance frequency. The dual band HMSAs by cutting the pair of rectangular slots or U-slot are proposed. The E-shaped HMSA was analyzed for the effects of the slots on the dual band response. The slot does not introduce any mode but reduces the second order mode resonance frequency of HMSA and along with the fundamental mode realizes dual band response. By studying the surface current distributions the resonance frequency formulations for the fundamental and the slot mode is proposed. The frequencies obtained using the proposed formulation closely agrees with the simulated values with a % error less than 5%.

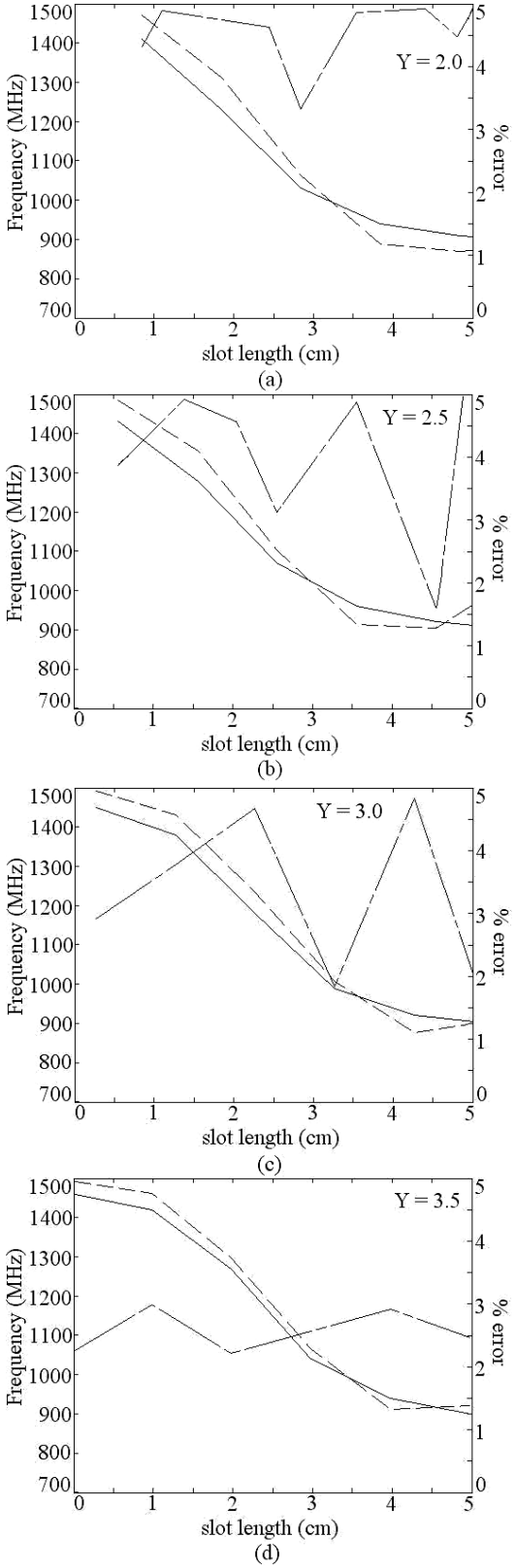

Figure 18 (a, b) Resonance frequency and % error plots at f_2 for E-shaped HMSA, (—) IE3D, (– –) calculated, (— - —) % error

7. REFERENCES

[1] G. Kumar and K. P. Ray, 'Broadband Microstrip Antennas', Artech House, USA, 2003.

[2] R. Garg, P. Bhartia, I. J. Bahl and A. Ittipiboon, Microstrip Antenna Design Handbook, Artech House, London, 2001

[3] B. Bhartia and I. J. Bahl, *Microstrip Antennas*, USA, 1980

[4] K. P. Ray, V. Sevani and Amit A. Deshmukh, "Compact gap-coupled microstrip antennas for broadband and dual frequency operations", International Journal of *Microwave and Optical Technology*, vol. 2, no. 2, July 2007, pp. 193 – 202.

[5] G. Kumar and K. C. Gupta, "Broadband Microstrip Antennas Using Additional Resonators Gap-Coupled to the Radiating Edges", *IEEE Trans. Antennas Propagation,* vol. 32, December 1984, pp. 1375–1379.

[6] C. K. Anandan, P. K. Mohanan and K. G. Nair, "Broadband Gap-Coupled Microstrip Antenna", *IEEE Trans. Antennas Propagation,* vol. 38, 1990, pp. 1581–1586.

[7] Amit A. Deshmukh, K. P. Ray, Priyanka T., Mayank J., and Sneha L., "Dual Band H-shape Microstrip antennas", *Proceedings of ICTSM – 2011*, 25 – 27 February 2011, Mumbai, India

[8] Ray, K. P., and Kumar, G.: 'Tunable and dual band Circular Microstrip Antenna with stubs', IEEE Trans. Antennas and Propagation, 2000, 48, pp. 1036 – 1039

[9] Ray, K. P., and Kumar, G.: 'Circular Microstrip Antennas with double stubs', Proc. ISRAMT-99, Malaga, Spain, December 1999, pp. 381 – 384

[10] Deshmukh, A. A., and Kumar, G., 'Even mode Multi-port Network Model for slotted dual band Rectangular Microstrip Antennas', Microwave & Opti. Tech. Letters, 2006, 48, 4, 798 – 804.

[11] Zhong S. S., and Lo, Y. T., 'Single Element Rectangular Microstrip Antenna for Dual frequency operation', Electronics Letters, 1983, 19, (8), pp. 298 – 300,

[12] Tang, C. T., Chen, H. T. and Wong, K. L., 'Small Circular Microstrip Antenna with Dual frequency operation', Electronics Letters, 1997, 33, pp. 1112 – 1113

[13] IE3D 12.1, Zeland Software, Freemont, USA